Optimal use of data in parallel tempering simulations for the construction of kinetic models of biomolecular dynamics

Jan-Hendrik Prinz,[1,*] John D. Chodera,[2,†] Vijay S. Pande,[3,‡]

William C. Swope,[4,§] Jeremy C. Smith,[5,¶] and Frank Noé[6,**]

[1]*Institute for Scientific Computing (IWR),*

University of Heidelberg, Im Neuenheimer Feld 368,

69126 Heidelberg, Germany and DFG Research Center Matheon,

FU Berlin, Arnimallee 6, 14195 Berlin, Germany

[2]*Research Fellow, California Institute of Quantitative Biomedical Research (QB3),*

University of California, Berkeley, 260J Stanley Hall, Berkeley, California 94720, USA

[3]*Department of Chemistry, Stanford University, Stanford, CA 94305*

[4]*IBM Almaden Research Center, 650 Harry Road, San Jose, California 95120*

[5]*UT/ORNL Center for Molecular Biophysics,*

Oak Ridge National Laboratory P.O.Box 2008 Oak Ridge TN 37831-6164, USA

[6]*DFG Research Center Matheon, FU Berlin,*

Arnimallee 6, 14195 Berlin, Germany

(Dated: October 13, 2009)

Abstract

Recent work has demonstrated how the short physical trajectories generated in PT simulations of biomolecules can be used to construct Markov models describing biomolecular dynamics at each simulated temperature. While this approach describes the temperature-dependent kinetics, it does not make optimal use of all available PT data, instead estimating the rates at a given temperature using only data from that temperature. This can be problematic, as some relevant transitions or states may not be sufficiently sampled at the temperature of interest, but might be readily sampled at nearby temperatures. Further, the comparison of temperature-dependent properties can suffer from the false assumption of temperature uncorrelated statistical errors. We propose here a strategy in which by a simple modification of the parallel tempering protocol, the harvested trajectories can be reweighted, permitting data from all temperatures to contribute to the estimated kinetic model. The method reduces the statistical uncertainty in the kinetic model relatice to the single temperature approach and provides estimates of transition rates even for transitions not observed at the temperature of interest. Further, the method allows the kineticd to be estimated at temperatures other than those at which simulations were run. To illustrate the method, an application is presented to the conformational dynamics of the solvated terminally-blocked alanine dipeptide.

INTRODUCTION

Biological macromolecules are not static structures, but are driven by thermal motion and interactions with their molecular environment, undergoing conformational fluctuations and changing conformational states. The characterization of the statistical conformational dynamics of biomolecules is of central importance in biology and medicine. Often, a separation of timescales of characteristic dynamical relaxation times gives rise to the existance of metastable conformational states, such that the biomolecule remains in any one of these states for a long time before a rapid transition is made to another. A wealth of experimental data now supports the existence of such states, including NMR [1, 2], fluorescence emission [3, 4], energy transfer[5], correlation spectroscopy [6], and nonequilibrium perturbation experiments[4]. Developing a quantitative understanding of what gives rise to these conformational states and the interactions that govern their transitions will provide insight into how post-translational[JCS] Why post-translational? modification and noncovalent association can affect dynamics and function, and will have a significant impact on our understanding of many biological processes, such as signaling events, enzyme regulation, allostery, and drug design for conformationally flexible molecules.

Parallel tempering simulations have been a popular approach to overcoming the issue of convergence in molecular simluations by allowing the bath temperature to change as the simulation proceeds[7]. At the same time this approach permits an analysis of temperature dependence, which is especially interesting for comparisons with certain experimental results[8] (e.g. melting curves, heat capacities). Although parallel tempering has the drawback that unphysical replica trajectories are produced, the short physical

Newtonian trajectories in between these exchanges can furnish useful information. If the parallel tempering simulation is in equilibrium, these trajectories will also be in equilibrium, and will give us information about the dynamics of the system at the respective temperatures.

Markov models provide a way to model the slow conformational dynamics of biomolecules such as peptides and proteins based on short simulations [9–12]. In these models, generally, conformational states are envisioned as disjoint, but connected regions of configurational space. The biomolecule spends long times within individual regions before undergoing rapid stochastic transitions between regions. If a separation of timescales exists between fast motions within a region and slow (i.e. infrequent) transitions between regions, the inter-state dynamics can be well described by a Markov Model in discrete timesteps τ, where the coarse graining in time is necessary since the discretization in space prohibits us from trading arbitrarily fast relaxation processes. If the system is partitioned into its metastable states, τ is related to the time required to overcome internal barriers within each conformational state. However, it has been shown recently that τ can be reduced (and the quality of the model is enhanced) by using additional states which are no longer metastable[13].

Recently, Buchete and Hummer have constructed Markov models using the short physical trajectories generated from parallel tempering simulations[14], allowing both the thermodynamics and kinetics to be modeled over the range of temperatures simulated. However, if a complete description of dynamics across the entire thermally-accessible configurational space is desired, one quickly runs into problems if ise is made of trajectories only from the temperature of interest as some states that are sampled at other temperatures may not be well sampled at the temperature of interest[14]. Fur-

thermore, independently of issues of temperature dependence, the configurational space spanned over the full range of temperatures simulated is larger than that at any single temperature. Hence, one would like to make use of the data collected at all temperatures to characterize the kinetic behavior in all regions sampled over the full range of temperatures spanned by the parallel tempering simulation. This approach resembles that of equilibrium reweighting.

Here, we propose an approach for integrating data from all temperatures by making use of dynamical reweighting[15], allowing a continuous estimate of the transition probabilities at any temperature without requiring the assumption of any kinetic model (such as Arrhenius kinetics[12]) and taking advantage of the increased transition rates at higher (or for transitions with entropic barriers, lower) temperatures. Reweighting methods (such as multiple histogram reweighting[16, 17], WHAM[18, 19] and MBAR[15]) allow the use of samples collected from multiple distributions to provide an improved estimate of the expectation value of some property at the distribution of interest, and have been used extensively in the analysis of equilibrium thermodynamic properties in replica-exchange simulations[20].

Dynamical reweighting has recently been proposed as a way of estimating dynamical properties (such as correlation functions) using an asymptotically optimal estimator, and also provides an estimate of the statistical error[21]. Here, we show how dynamical reweighting can be used to estimate transition probabilities (and their statistical uncertainties) as a smooth function of temperature, making use of data from all temperatures. This has the advantage of producing estimates of transition probabilities at *any* temperature and permitting the computation of properties that depend on derivatives with respect to temperature (e.g. heat capacities), although the quality of this estimate

will clearly depend on the number of times the transition is observed at "nearby" temperatures.

We illustrate this approach for the standard test case of the terminally-blocked alanine dipeptide in explicit solvent. A Markov model constructed from short (6 ps) trajectories from each state has been previously shown to describe the kinetics of this system accurately at 302K[11]. The dipeptide system presents a challenge for estimators based on individual temperatures, because states exist with very high free energies relative to the most populated states, and these are poorly sampled at temperatures near 300 K, even though they dominate the long-time relaxation kinetics at this temperature. Finally, we determine whether using all the data using reweighting produces substantially improved kinetic models at this particular temperature and across the full range of temperatures in the parallel tempering simulation.

This paper is organized as follows: First we review the theory behind Markov models of multistate conformational dynamics. We then show how dynamical reweighting can be used to estimate temperature-dependent transition probabilities and rates for a given state decomposition. Finally, we illustrate the method by applying it to a six-state decomposition of an MD simulation of the terminally-blocked alanine dipeptide, and compare the results to different Bayesian estimates of transition probabilities obtained from a single temperature alone.

THEORY

Markov Models

Let Ω be the configuration space with a complete decomposition into M disjoint sets $\Gamma_i \in \Omega$ such that

$$\bigcup_{i=1}^{M} \Gamma_i = \Omega,\ \Gamma_i \cap \Gamma_j = \emptyset,\ \forall i \neq j;\ i,j \in \{1,\dots,M\}. \tag{1}$$

For convenience we also define indicator functions $\chi_i \in \{0,1\}$ by setting

$$\chi_i(\boldsymbol{q}) = \begin{cases} 1 & \text{if } \boldsymbol{q} \in \Gamma_i \\ 0 & \text{else} \end{cases} \tag{2}$$

i.e., the function equals one if $\boldsymbol{q}$ belongs to set i and zero otherwise. Based on this discretization of state space we can define a (row-stochastic) transition matrix $\mathbf{T}$ with conditional probabilities of jumping from state i to state j after a specified lagtime τ by setting

$$T_{ij}(\tau) \ :=\ \mathbb{P}(\chi_j(\boldsymbol{q}(t+\tau)) = 1 \mid \chi_i(\boldsymbol{q}(t)) = 1), \tag{3}$$

which then propagates a probability distribution $\boldsymbol{p} \in [0,1]^M$ with time step τ by

$$\boldsymbol{p}(t+\tau) = \boldsymbol{p}(t)\mathbf{T}(\tau). \tag{4}$$

We aim here to construct a time- and space-discrete Markov model that approximates the long-time dynamics of the system by virtue of

$$\boldsymbol{p}(t+k\tau) \approx \boldsymbol{p}(t)\mathbf{T}^k(\tau). \tag{5}$$

Eq. 5 is only an approximation due to the introduction of the coarse-graining Γ. It has been shown [13], that the approximation error by the discretization Γ can be made arbitrarily small, by either choosing more states or increasing the underlying lagtime τ. Thus

with an appropriate choice of states we can ensure a good approximation by a time- and space-discrete Markov model. Although this is a crucial step, the process of actually finding an optimal decomposition of state space is beyond the scope of this paper and discussed elsewhere [10, 22].

Estimating transition probabilities vs estimating transition rates

In many studies coarse-grained dynamics is formulated with the Master equation

$$\dot{\boldsymbol{p}}(t) = \boldsymbol{p}(t)\ \mathbf{K} \tag{6}$$

with a rate matrix $\mathbf{K}$. While $\mathbf{T}(\tau)$ can be straightforwardly estimated from a series of observed transitions at time step τ, $\mathbf{K}$ cannot because the inversion of the equation

$$\mathbf{T}(\tau) = \exp(\tau\mathbf{K}) \tag{7}$$

is not unique for stochastic matrices unless $\mathbf{T}(\tau)$ is positive definite, and even then it is numerically unstable. In the following we focus on the estimation of time-discrete transition probabilities.

Estimation from time-discrete trajectories

Consider a trajectory $\boldsymbol{q}(t)$ sampled at time intervals Δt and let τ be an integer multiple of Δt. We introduce $\tau_\Delta = \tau/\Delta t \in \mathbb{N}$ and $L_\Delta = L/\Delta t \in \mathbb{N}$ and define a time discrete trajectory $\mathbf{q} \in \Omega^{L_\Delta+1}$

$$\boldsymbol{q}_i = \boldsymbol{q}(i\Delta t) \in \Omega,\ i \in \{0, \ldots, L_\Delta\} \tag{8}$$

and the count matrix $\mathbf{N}(\tau)$ of independent observed transitions by

$$N_{ij}(\tau)\ =\ \frac{1}{\tau_\Delta} \sum_{n=0}^{L_\Delta-\tau_\Delta} \chi_i\left(q_n\right) \chi_j\left(q_{n+\tau_\Delta}\right) \tag{9}$$

Assuming Markovianity, the likelihood that a given transition matrix produces the observations stored in the count matrix $\mathbf{N}$ is

$$\mathcal{L}(\mathbf{T}) = \mathbb{P}(\mathbf{N}|\mathbf{T}) = \prod_{i,j=1}^{M} T_{ij}^{N_{ij}}. \tag{10}$$

As a representative we choose the unique transition matrix $\hat{\mathbf{T}}$ which maximizes this likelihood :

$$\hat{T}_{ij} = [\text{argmax } \mathcal{L}(\mathbf{T})]_{ij} = \frac{N_{ij}(\tau)}{\sum_k N_{ik}(\tau)}. \tag{11}$$

Alternatively, we can use the state-to-state time-correlation function $C_{ij}(\tau)$ given by

$$C_{ij}(\tau) \equiv \langle \chi_i(0)\, \chi_j(\tau) \rangle \tag{12}$$

which can be estimated in a similar fashion

$$\hat{C}_{ij}(\tau) = \frac{1}{L_\Delta - \tau_\Delta} \sum_{n=0}^{L_\Delta - \tau_\Delta} \chi_i(q_n)\chi_j(q_{n+\tau_\Delta}) \tag{13}$$

$$= \frac{\tau_\Delta}{L_\Delta - \tau_\Delta} N_{ij}. \tag{14}$$

The present dynamical model is based on Hamiltonian dynamics, which is time reversible and thus equilibrium molecular dynamics fulfills detailed balance in state space. Consequently, for trajectories that sample from equilibrium, the correlation matrix will converge to a symmetric form $C_{ij}(\tau) = C_{ji}(\tau)$. In this case, we can use the estimator

$$\hat{C}_{ij} = \frac{\tau_\Delta}{2(L_\Delta - \tau_\Delta)}(N_{ij} + N_{ji}) \tag{15}$$

and write the transition matrix in terms of the correlation matrix $\mathbf{C}$ as

$$\hat{T}_{ij}(\tau) = \frac{\hat{C}_{ij}(\tau)}{\sum_k \hat{C}_{ik}(\tau).} \tag{16}$$

Transition probabilities from dynamical reweighting

We now demonstrate how transitions observed at high temperatures can be used to infer knowledge about the transition probabilities at lower temperatures: For a canonical ensemble at inverse temperature $\beta = (k_B T)^{-1}$ the state-to-state correlation functions can be expressed as Boltzmann-weighted expectation functions

$$C_{ij}(\tau;\beta) \;=\; \frac{1}{Z(\beta)} \int d\boldsymbol{q}(0) d\boldsymbol{p}(0) \exp\left(-\beta \mathcal{H}(\boldsymbol{q}(0),\boldsymbol{p}(0))\right) \left(\chi_i(\boldsymbol{q}(0))\chi_j(\boldsymbol{q}(\tau))\right) \tag{17}$$

where $Z(\beta)$ is the complete partition function of both kinetic and potential part.

Suppose we have a set of N_k Hamiltonian trajectories $\boldsymbol{z}_{kn}(t)$, $n = 1, \ldots, N_k$, $t \in [0, T]$, in which the initial phase space points $\boldsymbol{z}_{kn}(0)$ are sampled from canonical (NVT) distributions at corresponding inverse temperatures β_k, $k = 1, \ldots, K$. By the application of *dynamical reweighting*[15] , a correlation function $C_{ij}(\tau;\beta)$ can be estimated using the entire set of trajectories at all temperatures as

$$\hat{C}_{ij}(\tau;\beta) \;\approx\; \sum_{k}^{K} \sum_{n}^{N_k} w_{kn}(\beta) \cdot \hat{C}_{ij}^{(kn)}(\tau) \tag{18}$$

where the individual microcanonical contributions to the correlation functions are given by Eq. (15)

$$\hat{C}_{ij}^{(kn)} = \frac{\tau_\Delta}{2(L_\Delta - \tau_\Delta)} \left(N_{ij}^{kn} + N_{ji}^{kn}\right) \tag{19}$$

The row-stochastic transition matrix estimate $\hat{\mathbf{T}}(\tau;\beta)$ is then estimated from (16)

$$\hat{T}_{ij}(\tau;\beta) \;=\; \frac{\hat{C}_{ij}(\tau;\beta)}{\sum_k \hat{C}_{ik}(\tau;\beta)} \tag{20}$$

As $\hat{\mathbf{C}}(\tau;\beta)$ is symmetric by construction, $\hat{\mathbf{T}}(\tau;\beta)$ will be reversible.

The normalized trajectory weights $w_{kn}(\beta)$ are specified in terms of unnormalized

weights, which can be computed by

$$w_{kn}(\beta) \;=\; \tilde{w}_{kn}(\beta) / \sum_{k=1}^{K} \sum_{n=1}^{N_k} \tilde{w}_{kn}(\beta) \tag{21}$$

$$\tilde{w}_{kn}(\beta) \;=\; \left[\sum_{k'=1}^{K} N_{k'} \, \exp[\hat{f}_{k'} - (\beta - \beta_{k'}) \, E_{kn}] \right]^{-1} \tag{22}$$

where $E_{kn} \equiv H(\boldsymbol{z}_{kn}(0))$ denotes the total energy of the trajectory, which is constant over trajectories for Hamiltonian dynamics. The dimensionless free energies $\hat{f}_i = -\ln Z_i + c$ are determined by the solution of a set of self-consistent equations

$$\hat{f}_i \;=\; -\ln \sum_{k=1}^{K} \sum_{n=1}^{N_k} \tilde{w}_{kn}(\beta_i), \;\; \forall \; i \in \{1, \ldots, K\} \tag{23}$$

which can be obtained efficiently by a number of means [15], although it is often necessary to work with logarithmic representations to avoid numerical instability. A complete derivation of all expressions above is presented in Ref. [21].

Estimation of uncertainties in transition probabilities

The statistical uncertainty in $\hat{C}_{ab}(\tau, \beta)$ can be estimated in a straightforward manner using the machinery of MBAR [15]. We following the derivation presented in [21] and first reindex k and n in the datasets $\{\boldsymbol{z}_{kn}, E_{kn}, \hat{C}_{ab,kn}\}$ by replacing it with one single index $n = 1, \ldots, N$, where $N = \sum_{k=1}^{K} N_k$ and $a, b = 1, \ldots, M$ with $M = 6$ being the number of states in the model considered. This results in the datasets $\{\boldsymbol{z}_n, E_n, \hat{C}_{ab,n}\}$.

We form the $N \times (K + 1 + M^2)$ matrix W_{nk} such that

$$W_{nk} = \begin{cases} \exp[-\beta_k E_n] & k = 1, \ldots, K \\ \exp[-\beta E_n] & k = K + 1 \\ \hat{C}_{ab,n} \, \exp[-\beta E_n] & \begin{array}{l} k = K + 1 + a(M-1) + b, \\ a, b = 1, \ldots, M \end{array} \end{cases} \tag{24}$$

The uncertainty of the transition probabilities $T_{ij}(\hat{C}_{11}, \ldots, \hat{C}_{MM})$ can then be estimated by

$$\begin{aligned} \delta^2 T_{ij} &\equiv \left\langle (T_{ij} - \langle T_{ij} \rangle_\beta)^2 \right\rangle_\beta \\ &\approx \sum_{a=1}^{M} \sum_{a'=1}^{M} \sum_{b=1}^{M} \sum_{b'=1}^{M} \left[\frac{\partial T_{ij}}{\partial \hat{C}_{ab}} \right] \left[\frac{\partial T_{ij}}{\partial \hat{C}_{a'b'}} \right] \delta \hat{C}_{ab} \delta \hat{C}_{a'b'} \end{aligned} \tag{25}$$

where the covariance of the estimates $\hat{C}_{ab}$ and $\hat{C}_{a'b'}$ can be estimated as

$$\begin{aligned} \delta \hat{C}_{ab} \delta \hat{C}_{a'b'} \;\approx\; & \hat{C}_{ab}\, \hat{C}_{a'b'} [\hat{\Theta}_{K+1,K+1} + \hat{\Theta}_{K+1+a(M-1)+b,K+1+a'(M-1)+b'} \\ & - \hat{\Theta}_{K+1,K+1+a'(M-1)+b'} - \hat{\Theta}_{K+1+a(M-1)+b,K+1}] \end{aligned} \tag{26}$$

with covariance matrix $\hat{\mathbf{\Theta}} = [(\mathbf{W}^{\mathrm{T}}\mathbf{W})^{+} - \mathbf{N}]^{+}$ and $\mathbf{N} = \mathrm{diag}(N_1, \ldots, N_K, 0, \ldots, 0)$. The $[]^{+}$ here denotes the generalized inverse. Using Eq. (3) the sensitivity of T_{ij} to the correlation $\hat{C}_{ab}$ is given by

$$\frac{\partial T_{ij}}{\partial \hat{C}_{ab}} = \frac{\delta_{aj}\delta_{bi} + \delta_{ai}\delta_{bj} - \delta_{ab}}{\hat{C}_i} - \frac{\hat{C}_{ij}\,(-M\delta_{ab} + \delta_{ai} + \delta_{bi})}{\hat{C}_i^2}, \tag{27}$$

leading to a complex but still enumerable expression for the diagonal entries in the covariance matrix of transition probabilities $\delta^2 T_{ij}$. A more thorough derivation of the above can be found in [15, 21].

Modified parallel tempering protocol

By using a modified parallel tempering protocol, a set can be generated of Hamiltonian trajectory segments $\boldsymbol{z}_{kn}(t)$ of uniform length $T \geq \tau$ the initial phase space points $\boldsymbol{z}_{kn}(0)$ of which are sampled from the canonical (NVT) ensemble at corresponding inverse temperatures $\beta_1, \ldots, \beta_K$.

We start by assuming that some process was used to generate the initial phase space points $\boldsymbol{z}_{k0}(0)$ from equilibrium at each corresponding inverse temperature β_k

$$\boldsymbol{z}_{k0}(0) \;\sim\; [Z(\beta_k)]^{-1}\, e^{-\beta \mathcal{H}(\boldsymbol{z}_{k0}(0))} \tag{28}$$

This initial phase space point generation maz be by menans, for example, of a standard parallel tempering protocol, or by running the modified protocol for a number of iterations starting from a single configuration.

Consider iteration n of the algorithm. For each temperature index $k = 1, \ldots, K$, Hamilton's equations of motion are propagated using a symplectic integrator to generate trajectories of $\boldsymbol{z}_{kn}(t)$ of length T. Finally, we propose exchanges[11] between the final configurations $\boldsymbol{z}_{in}(T)$ and $\boldsymbol{z}_{jn}(T)$ of neighboring temperatures β_i and $\beta_{i\pm1}$, starting from the highest temperature down to the lowest one in odd iterations and in reverse order in even ones. The Metropolis-like probability[7] of accepting or rejecting the exchange depends on the final potential energies of the configurations U_i and U_j with

$$P_{\text{exch}}(U_i, \beta_i; U_j, \beta_j) \;=\; \min\{1, \exp[-(\beta_i - \beta_j)(U_j - U_i)]\}$$

Regardless of whether the exchange is accepted or rejected, we reassign the velocities according to the Maxwell-Boltzmann distribution at the new (old) temperatures, and denote the new phase space points from which the next iteration can be carried out as $\boldsymbol{z}_{k(n+1)}(0)$ (see proof in Appendix). This satisfies the conditions defined by Okamoto[7] in order for the kinetic energies to not appear in P_{exch}. The reason for reassigment of velocities instead of rescaling is that, when using Hamiltonian trajectories no thermostating would otherwise take place.

Bayesian estimate of transition probabilities from a single temperature

To analyze how the combination of data from all temperatures reduces the uncertainty in the estimation of the transition matrix estimates we compare the present method to two Bayesian methods of error estimation working on data only at a single temperature.

Both Bayesian methods sample transition probabilities or rates according to the same likelihood function, but employ different proposal steps and, more importantly different prior probability distributions.

Let $N_{ij}(\tau, \beta)$ be the transition counts from all trajectories at inverse temperature β. Then the a posteriory probability of transition matrix T_{ij} given this observation is

$$\mathbb{P}(\mathbf{T}|\mathbf{N}) \propto \mathbb{P}(\mathbf{T})\, \mathbb{P}(\mathbf{N}|\mathbf{T}) = \mathbb{P}(\mathbf{T}) \prod_{i,j \in S} T_{ij}^{N_{ij}}. \tag{29}$$

As the prior $\mathbb{P}(\mathbf{T})$ we choose a Dirichlet distribution for each row which adds no additional observations to the likelihood probability

$$\mathbb{P}(T) \equiv \prod_{i,j \in S} T_{ij}^{-1}. \tag{30}$$

Furthermore, we restrict ourselves to transition matrices that fulfill detailed balance, i.e., are reversible with respect to the stationary distribution π:

$$\pi_i T_{ij} = \pi_j T_{ji} \tag{31}$$

Here, the distribution in Eq. (29) was sampled using a Markov chain Monte-Carlo procedure described in Ref. [23]. The approach proposed in Ref. [14] does not estimate the transition probabilities directly, but uses a likelihood function based on parameters of a reversible rate matrix $\mathbf{K}$ with the corresponding likelihood

$$\mathbb{P}(\mathbf{K}|\mathbf{N}) \propto \mathbb{P}(\mathbf{K}) \prod_{i,j \in S} \exp\left(\tau \mathbf{K}\right)_{ij}^{N_{ij}} \tag{32}$$

and the detailed balance constraint

$$\pi_i K_{ij} = \pi_j K_{ji}. \tag{33}$$

The choice of parametrization for $\mathbf{K}$ in Ref. [14] stores the logarithms of the upper-right triangular matrix (without diagonal entries) and the equilibrium distribution, thus assuring a rate matrix with negative eigenvalues and also positive off-diagonal rates. After

Transition Matrix Estimation [23]	[TE]	RED
Rate Matrix Estimation [14]	[RE]	GREEN
Dynamical Reweighting [21]	[DR]	BLUE
Shooting Trajectories at 302K [11]	[ST]	BLACK

TABLE I: Table of methods used for transition probability or rate estimation with their corresponding abbreviations and colors used consitently thoughout this paper

sampling rate matrices with a Metropolis-Monte Carlo scheme the related set of transition matrices with the lagtime τ is computed by

$$\mathbf{T} = \exp\left(\tau \mathbf{K}\right) \tag{34}$$

All methods with their abbreviations and colors used consistently in the text and figures in this article are listed in Table I Do we really need this?.

APPLICATION TO TERMINALLY-BLOCKED ALANINE DIPEPTIDE

System Setup

To illustrate the dynamical reweighting method described above, we apply it to estimate transition probabilities between conformational states for the terminally-blocked alanine peptide (Ace-Ala-Nme).

For the analysis a parallel tempering dataset for the terminally-blocked alanine peptide in a box of 431 TIP-3P water molecules was generated as described previously [11]. The parallel tempering simulation was conducted according to the modified protocol described in the theory section generating an ensemble of 501 Hamiltonian trajectories of 20

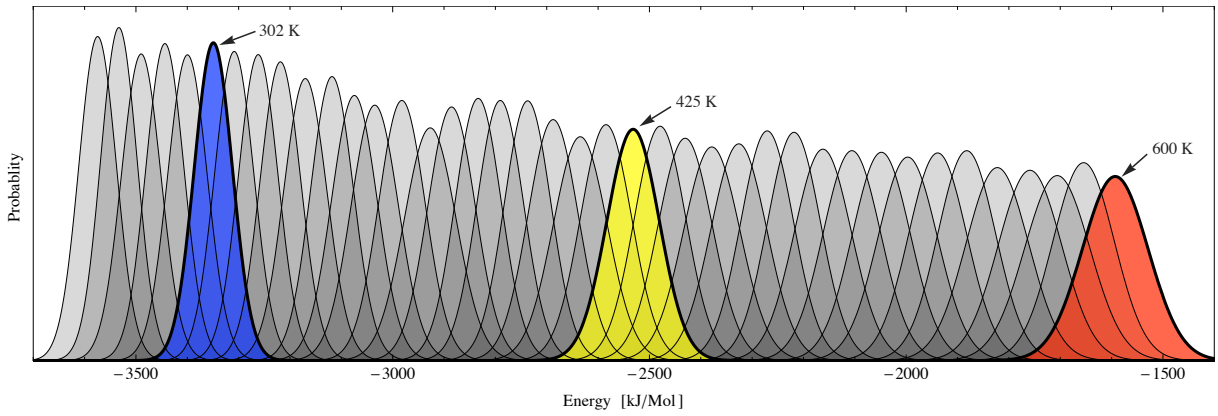

FIG. 1: Distribution of energies in the trajectories in kJ/mol for all 40 temperatures. Highlighted are temperatures 302 K, 426 K and 600 K to allow reference with convergence properties in Figure 8. The temperature spacing was chosen as exponential so as to provide an average overlap of $\sim 50\%$ between neighboring temperatures.

ps length at each of 40 temperatures spanning 273 to 600 K, with peptide configurations stored every 0.1 ps. The temperatures were exponentially spaced, thus providing good overlap in the potential and total energy distributions between neighboring temperatures and resulting in an average exchange acceptance probability of $\sim 50\%$ (see Figure 1).

A velocity Verlet integrator[24] (with bonds involving hydrogen atoms constrained) was used to produce the dynamical trajectories. The fluctuations in total energy over the 20 ps trajectories was minimal and the drift negligible (see Table II). The production run followed a 1 ns equilibration phase, ensuring that all initial configurations were drawn from equilibrium at their respective temperatures. Previous work has demonstrated that a Markov model based on a six-state decomposition as depicted in Figure 2 can accurately describe the dynamics of this peptide for lagtimes longer than $\tau = 6$ ps[11]. In order to conveniently directly apply the reweighting procedure we used the same state

Temp [K]	RMS [J/mol]	rel. RMS	Drift [J/(ps mol)]	rel. Drift [1/ps]
302	214.844 ± 0.648	$6.41 \cdot 10^{-5}$	0.608 ± 0.249	$1.82 \cdot 10^{-7}$
600	26.617 ± 0.083	$1.67 \cdot 10^{-5}$	1.061 ± 0.432	$6.66 \cdot 10^{-7}$

TABLE II: RMS and Drift of Energies over 20ps trajectories

decomposition for all temperatures.

To evaluate the accuracy of the methods for estimating transition probabilities, we compare the separate estimates from (DR),(TE) and (RE) to a reference simulation of 6x10000 short, 10 ps trajectories shot out of the equilibrium of each state at 302 K. The PT simulation in comparison furishes a total of 1500 independent transitions shared between all states at that temperature, which means that the shooting dataset has 40 times more observations compared to the PT simulation, thus providing a statistically reliable reference.

The system is small enough such that a reasonable statistics can be obtained with moderate CPU requirements while at the same time being complex enough such that some transitions (and even some states) are sampled only at high temperatures. In what follows, the results from the Markov model obtained from the dynamical reweighting method are compared to the model computed by Bayesian analyses using data from a single temperature only.

Estimated transition probabilities as a function of temperature

A comparison of the transition probabilities between all 6x6 pairs of states as a function of temperature is given in Figure 3. The blue solid lines give the estimates from

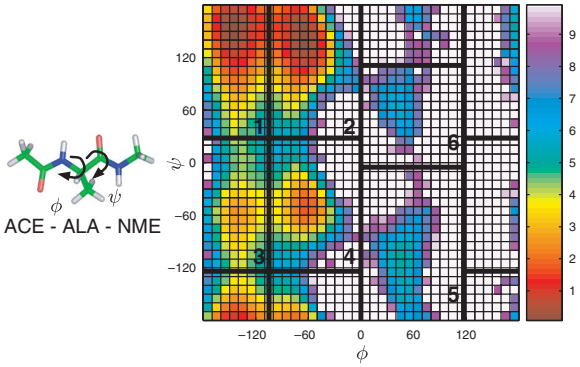

FIG. 2: Terminally-blocked alanine potential of mean force and state boundaries. Left: The terminally blocked alanine peptide with (ϕ, ψ) torsions labeled. Right: The potential of mean force as a function of (ϕ, ψ) torsions at 302 K in units of $k_B T$ estimated from the parallel tempering simulation using WHAM[18, 25], truncated at $10 k_B T$ (white regions). The six manually identified states are labelled in black[11].

dynamical reweighting (DR)[11] using all available data at all temperatures as described in the Theory section. To obtain the dimensionless free energy estimates $\hat{f}_i$ we solved the set of self-consistent equations in (23) with a relative convergence tolerance in the residual of 10^{-7}. Transition probabilities were also estimated at one intermediate temperature between each pair of simulated temperatures.

The red dashed lines in Figure 3 show transition probabilities for the reversible single temperature estimation of transition matrices (TE)[23]. For each of the 40 temperatures the sampler was run to collect a total of 10,000 samples. For the sampling of reversible rate matrices (RE), depicted by dotted green lines, the sampling as proposed in Ref. [14] was used. After an equilibration phase again a total of 10,000 samples were stored for each temperature separately. For the convergence of both methods see supplementary Figure 8. The black cross-hair in Figure 3 refers to the reference values at

302 K. Qualitatively all methods agree, especially in the lower energy states (1 to 4). However, the reweighting estimate, which uses the combined data from all temperatures, has smaller uncertainties than the estimators that use only individual temperatures. The overall agreement with the reference simulation is best for dynamical reweighting. The two Bayesian methods have almost identical predictions for states with many observed transitions, which is as expected since they use the same likelihood functions and the influence of the choice of the prior probaility distribution is minimal here. However, the differences in the states with few observations (states 5 and 6) arise from the influence of different prior probability distributions.

Detailed comparison of transition probability estimates at 302 K

For a detailed comparison the Bayesian analysis method with reversibility constraint for transition matrices[23] (TE) was applied to the set of shooting trajectories at 302 K as well to generate an estimate of reference transition probabilities obeying detailed balance. The results of the comparison at 302 K between the different estimation methods are shown in Figure 4. All colors are the same as in Figure 3.

For transitions that are not sampled at certain temperature ranges, the maximum-likelihood estimates obtained with the present reweighting method are close to zero (see Figure 3). Generally, for transition probabilities close to zero or one the normal distribution is a poor approximation to this highly asymmetric distribution and therefore leads to too large uncertainties (see Figure 4) in cases. Thus we suspect that reweighting will significantly overestimate the uncertainty in these cases since this is derived from the locally estimated Hessian of the probability distriution.

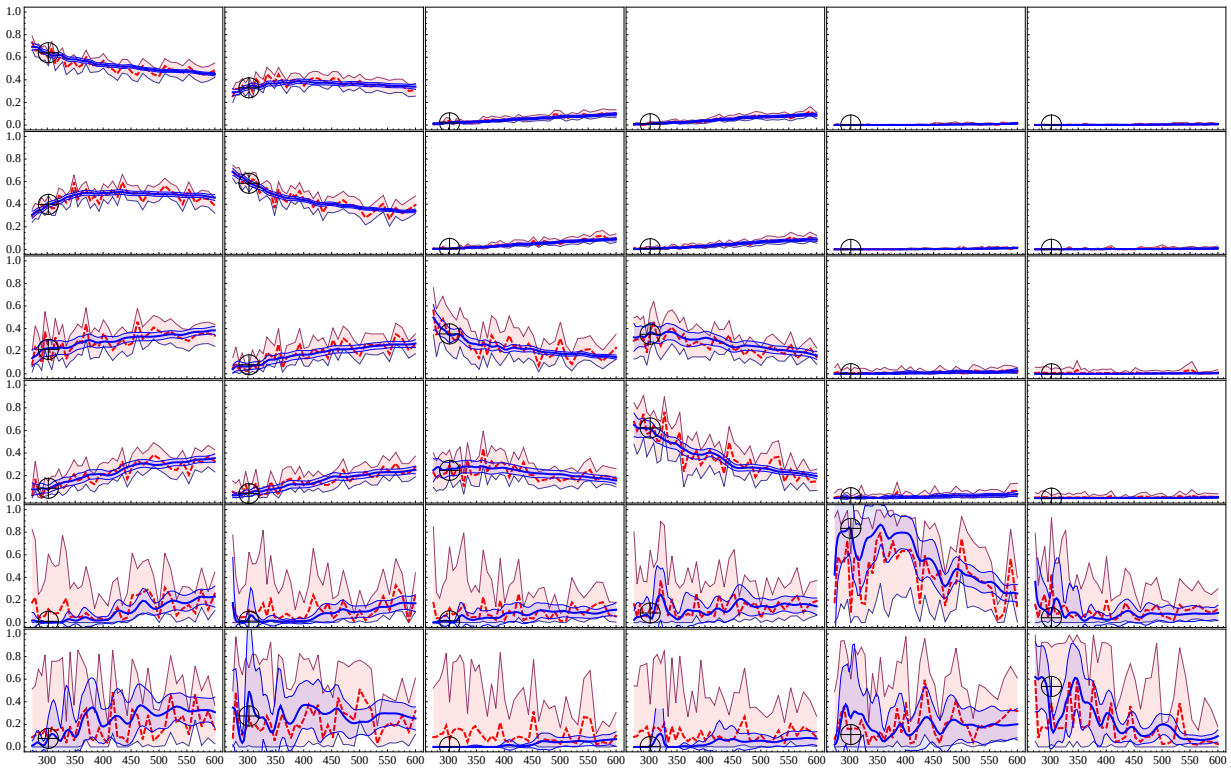

FIG. 3: Comparison of all 6x6 inter-state transition probabilities as a function of temperature with error bars showing 95% confidence intervals. Blue lines show the transition probabilities estimated using the present method (DR). Red lines show the estimates from transition matrix estimation (TE) computed from only single temperature data. The black cross-hair indicates the reference using the shooting trajectory data (ST) at 302K only. It is apparent that the reweighting method provides useful and bounded estimates across the whole temperature range even at temperatures where the corresponding transition was not observed (e.g., at transitions from state 5 and 6 for low temperatures). The Bayesian counting method without reweighting is very noisy and not useful in situations at low temperatures for transitions with poor statistics.

The reweighting method performs overall very well compared to the single-temperature estimates. Even transition probabilities that are sampled very poorly at 302 K (such as for transitions involving states 5 and 6) have a good agreement with the

	Variance in Estimation		
	(DR)	(TE)	(RE)
Low-energy states (1 to 4)	0.007	0.023	0.055
High-energy states (5 and 6)	0.140	0.267	0.288
All Transitions	0.079	0.151	0.167

TABLE III: Standard Deviation in the absolute difference of transition probabilities compared to the reference simulation (ST) at 302K for the three methods of Markov model estimation and high- and low-energy subsets of transitions. Dynamical reweighting (DR) shows the smallest spread in deviation from the reference simulation (ST).

reference values at 302 K. Table III shows the standard deviation in the absolute difference of the estimation methods compared to the reference simulation (ST). The dynamical reweighting has a smaller deviation than both Bayesian methods for both high- and low-energy states.

Comparison of temperature dependence of eigenvalues

Dynamical reweighting can also be applied to estimate properties derived from the transition probabilities. For example, the eigenvalues λ_i of a transition matrix are related to the timescales of processes t_i^* indicated by the corresponding eigenvector by

$$t_i^* = -\tau / \log(\lambda_i). \tag{35}$$

Hence, eigenvalues close to one imply slow processes i.e., those we are mostly interested in. We investigated the dependence of the eigenvalues on the temperature in the present

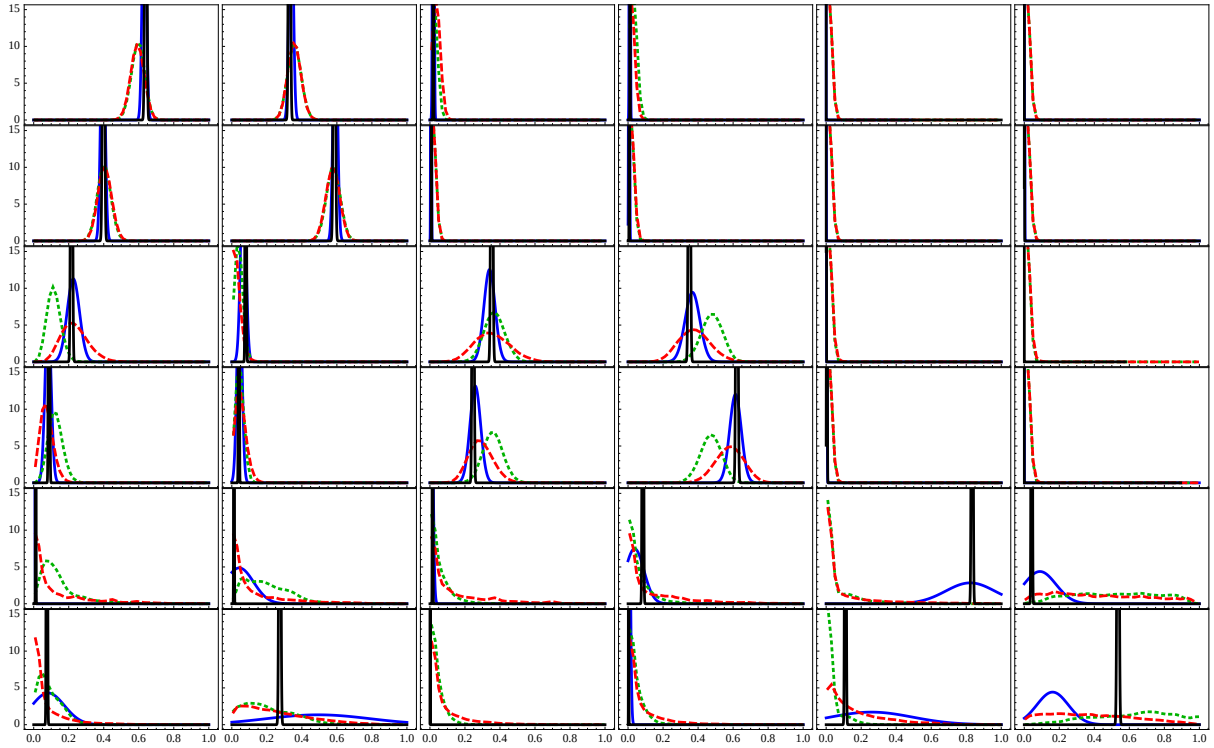

FIG. 4: Detailed Comparison of transition probabilities at 302 K. Red: Single temperature estimation of transition matrix (TE), Green: Single temperature estimation of rate matrix (RE), Blue: dynamical reweighting estimation (DR), Black: reference using shooting trajectories (ST).

system. Figure 5 compares estimates for the second and third eigenvalue λ_2, λ_3 of the transition matrix estimated at each temperature with the different methods. The variance in the TE case was estimated from the set of eigenvalues of each sampled transition matrix. To estimate the errors of DR we used linear error propagation of the uncertainties in the transition matrix to the errors in the eigenvalues [26]. At low temperatures, the second eigenvalue is estimated correctly by dynamical reweighting (DR), but not by single-temperature estimations. This is due to the fact that the transition process corresponding to this slowest timescale is not sampled at these low temperatures. Thus, estimates using only data collected at that temperature are errorneous. The agreement of dynamical

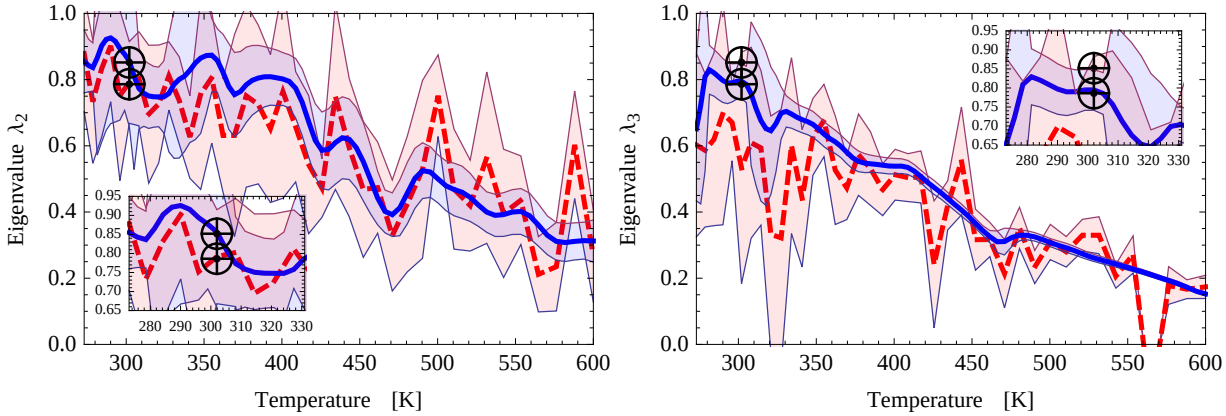

FIG. 5: Red: Single temperature estimation of transition matrix (TE), Blue: dynamical reweighting estimation (DR), Black: reference using shooting trajectories (ST). Left: Comparison of the second eigenvalue vs temperature, Right: Comparison for third eigenvalue. The third eigenvalue is well predicted by both estimation methods at all temperatures, while the second eigenvalue at low temperatures is only detected by dynamical reweighting.

reweighting timescales with the reference simulation is very good, although the error bars of the reweighted estimate are still very large compared the good agreement of the expectation values with the reference. We assume that the inappropriate approximation of the asymmetric distributions with normal distributions used for the linear error propagation lead here as well to an overestimation of the errors in the transition probabilities.

The third largest eigenvalue is predicted by both methods equally well (Fig. 5). Although this was found as the second-largest eigenvalues in the single-temperature estimates, which missed sampling the slowest process completely. A direct comparison of the predicted eigenvectors (Fig. 6) reveals that the slowest process (given by the second eigenvector of the reference transition matrix (ST)) is not detected by any of the single temperature methods. However, Dynamical reweighting successfully finds all the processes, although the matching eigenvalues and thus timescales are mixed up for faster

processes. The comparison of Markov Models is a nontrivial task, for which we used a symmetrized form of the transition matrix $\mathbf{T}^{sym}$ and expand it into a sum of rank one matrices $\mathbf{Q}_i$ spanned by an outer product of the eigenvectors of $\mathbf{T}^{sym}$ by

$$\begin{aligned}
\mathbf{T}^{sym} &= \mathrm{diag}(\boldsymbol{\pi}^{1/2})\ \mathbf{T}\ \mathrm{diag}(\boldsymbol{\pi}^{-1/2}) && (36)\\
&= \mathbf{R}\ \mathrm{diag}(\boldsymbol{\pi}^{1/2})\ \mathbf{R}^{\mathbf{T}} && (37)\\
&= \sum_{i=1}^{M} \lambda_i \boldsymbol{r}_i\ \boldsymbol{r}_i^T && (38)\\
&= \sum_{i=1}^{M} \mathbf{Q}_i. && (39)
\end{aligned}$$

Here, $\boldsymbol{\pi} = \{\pi_1, \ldots, \pi_M\}$ is the equilibrium distribution, $\mathbf{R} = \{\boldsymbol{r_1}, \ldots, \boldsymbol{r_M}\}$ the matrix of eigenvectors of $\mathbf{T}^{sym}$ and λ_i the corresponding eigenvalues, which are equal to the eigenvalues of $\mathbf{T}$. Each of the submatrices $\mathbf{Q}_i$ can be considered as a part of the full transition matrix working on a timescale given by the respective eigenvalue. These subprocesses are similar if their eigenvectors match, as can be determined by the scalar product.

Contributions from different temperatures to the estimates of expectation values

The contribution of each trajectory snippet to the estimation of any expectation value at any given temperature is illustrated in Fig. 7. The left plot shows the average normalized weights

$$\bar{w}_{kl} = \frac{1}{N_k} \sum_n w_{kn}(\beta_l) \tag{40}$$

given in (22), where, on average, seven temperatures contribute more than 1% to the expectation. The right hand plot illustrates the contribution to the transition counts N_{65}

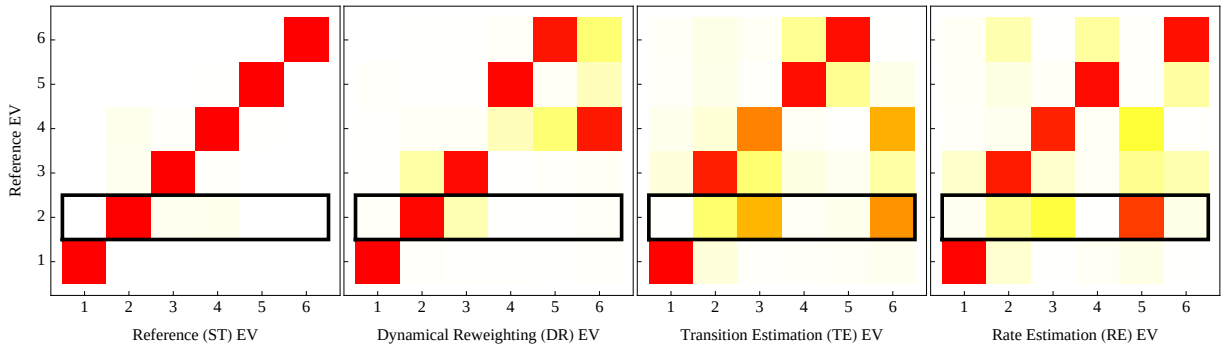

FIG. 6: Similarity matrices (scalar product) of eigenvectors from symmetrized transition matrices estimated with different methods (ST, DR, TE, RE) at 302 K. The eigenvectors indicate the states involved in the process, thus high similarity (red) indicates a good approximation to the reference process (ST). Eigenvectors are sorted as descending eigenvalues. The 2nd eigenvector is found correctly only by dynamical reweighting, meaning that the single temperature estimations are unable to correctly predict the slowest process at 302 K.

for the transition $6 \rightarrow 5$ given by

$$\frac{1}{N_k} \sum_{n=1}^{N_k} \tilde{w}_{kn}(\beta_l) \hat{C}_{ij}^{kn}, \tag{41}$$

with k indicating the temperature contributed from, l the temperature estimated at and i, j representing the transition $i \rightarrow j$. As expected most information contributing to a specific temperature estimate is always contained in the simulations performed at the nearest temperatures.

DISCUSSION

The present method provides a means of generating an estimate of transition probabilities from parallel tempering MD simulations of biomolecules as a continuous function

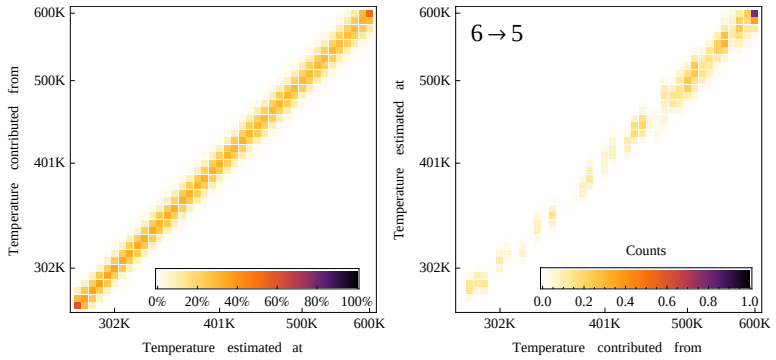

FIG. 7: Left: Relative contribution $\bar{w}_{kl}$ in Eq. 40 to the estimates at inverse temperature β_k from simulations at inverse temperature β_l averaged over all trajectories at the same temperature. On average, 7 temperatures contribute more than 1% each to the estimation. Right: Contributions to the estimation of transition counts for the transition $6 \to 5$. The sum of one row equals to the total counts estimated by the method at the desired temperature.

of temperature. Even at intermediate temperatures not simulated at, the error bars are much smaller then obtained with either single-temperature methods. At low temperatures, where some transitions are not observed at all, non-zero transition probabilities can still be estimated.

Additionally, the method allows to differentiation of the estimates of transition probabilities with respect to the inverse temperature β, because the trajectory weights $w_{kn}(\beta)$ are differentiable functions with respect to temperature (22). This allows, in principle, thermodynamic properties to be computed (e.g., heatcapacities), although these quantities are in general numerically difficult to handle, since the trajectory weights can easily span hundreds of orders of magnitude.

The method requires a set of parallel tempering simulations with a modified protocol to produce a series of NVE trajectories with initial configurations drawn from the NVT ensemble. For very large systems, the PT simulation might not be long enough to glob-

ally converge. In this case we cannot use reversible counting as in Eq. (19) to enhanced the statistics, but the method can still be applied without the detailed balance constraint as long as we draw from equilibrium inside each set Γ_i. The PT requirement of good exchange rates also ensures good overlap in the contribution to the dynamical reweighting for neighboring temperatures. The approach itself is not limited to Hamiltonian trajectories but can be extended to other dynamics as long as an analytical connection between the weighting factors and the temperature exists (e.g. Boltzmann distributed probabilities)[21]. For example, this is the case for Brownian and Langevin dynamics.

The degree to which the use of parallel tempering can speed up convergence is a matter of discussion. [JCS] Needs: References While activated processes will be sampled more often at higher temperatures, entropic barriers become less and less probable to pass, effectively limiting the possible increase in simulation speed. The same problem limits the range of contributing temperatures here, too. Nevertheless, information about activated processes is transferred from higher to lower temperatures and, for entropic barriers from lower to higher temperatures. Transitions in the alanine peptide are dominated by activated processes (i.e., enthalpic barriers).

Both single-temperature methods give quite similar results for transitions with good statistics, differing mostly for transitions that have only rarely been sampled due presumably to the influence of different prior probability distributions. Surprisingly, the Bayesian estimates provide a reasonable bound on transition probabilities to and from a state even when the state is not even sampled. This is most likely due to the reversibility constraint, which seems to provide information even in cases where there are few transitions to or from a state.

There is, however, a dependence on the prior, which leads to different predictions

in cases where the state is not or only rarely sampled. The rate matrix estimation (RE) assumes, in addition to the detailed balance constraint, positivity of all eigenvalues and non-negative off-diagonal entries. The uniform distribution of parameters in logarithmic space leads most likely to favoring of small transition probabilities in states with poor transition statistics.

The way in ehich the transition probabilities are estimated in terms of equilibrium correlation functions requires that the trajectory segments sampled during the parallel tempering simulation are drawn from the equilibrium distribution and that the trajectories to be reweighted are uncorrelated so as to permit an estimation of the statistical error.

The predictions of mean values are very good, while the quality of the error estimation is limited to a Gaussian approximation, which is problematic in cases where transition probabilities are close to 0 or 1 and the probability distribution is thus very asymmetric. Some combination of Bayesian and reweighting methods (such as T-WHAM[19]) may provide the best of both types of estimators by yielding more accurate uncertainties at the expense of introducing some bias from the introduction of energy histograms. Finally, the enhanced estimates of mean values and their respective statistical uncertainties may be used to guide subsequent (potentially adaptive) sampling strategies, as described in Ref. [27].

ACKNOWLEDGMENTS

The authors would like to thank Jed W. Pitera (IBM Almaden), Nicolae-Viorel Buchete (UCD Dublin) and Gerhard Hummer (NIH) for stimulating conversations during the execution of this work. JHP gratefully acknowledges funding from the German Re-

search Foundation (DFG) through the award of a doctoral scholarship in the International Graduiertenkolleg IGK 710: "Complex processes: Modeling, Simulation and Optimization". JDC gratefully acknowledges support from HHMI and IBM predoctoral fellowship programs, NIH grant GM34993 through Ken A. Dill (UCSF), and NSF grant for Cyberinfrastructure (NSF CHE-0535616), and a California Institute for Quantitative Biosciences (QB3) Distinguished Postdoctoral Fellowship at various points throughout this work. JHP and FN acknowledge support from DFG Research Center Matheon. JCS acknowleges funding from the U.S. Department of Energy "Multiscale Mathematics" Grant No. missing!

* Electronic address: jan-hendrik.prinz@iwr.uni-heidelberg.de

† Corresponding author; Electronic address: jchodera@berkeley.edu

‡ Electronic address: pande@stanford.edu

§ Electronic address: swope@almaden.ibm.com

¶ Electronic address: smithjc@ornl.gov

** Electronic address: noe@math.fu-berlin.de

[1] E. Z. Eisenmesser, D. A. Bosco, M. Akke, and D. Kern, Science **295**, 1520 (2002).

[2] E. Z. Eisenmesser, O. Millet, W. Labeikovsky, D. M. Korzhnev, M. Wolf-Watz, D. A. Bosco, J. J. Skalicky, L. E. Kay, and D. Kern, Nature **438**, 117 (2005).

[3] W. Min, G. Luo, B. Cherayil, S. Kou, and X. Xie, Phys. Rev. Lett **94**, 1 (2005).

[4] G. Smith, K. Lee, X. Qu, Z. Xie, J. Pesic, T. Sosnick, T. Pan, and N. Scherer, J. Mol. Biol. **378**, 941 (2008).

[5] X. Zhuang and M. Rief, Curr. Opin. Struct. Biol. **13**, 88 (2003).

[6] H. Neuweiler, S. Doose, and M. Sauer, Proc. Nat. Acad. Sci. USA **102**, 16650 (2005).

[7] Y. Sugita and Y. Okamoto, Chem. Phys. Lett. **314**, 141 (1999).

[8] M. Jäger, H. Nguyen, J. C. Crane, J. W. Kelly, and M. Gruebele, J. Mol. Biol. **311**, 373 (2001).

[9] N.-V. Buchete and G. Hummer, J. Phys. Chem. B **112**, 6057 (2008).

[10] F. Noé, I. Horenko, C. Schütte, and J. C. Smith, J. Chem. Phys **126**, 155102 (2007).

[11] J. D. Chodera, W. C. Swope, J. W. Pitera, and K. A. Dill, Multiscale Model. Sim. **5**, 1214 (2006).

[12] S. Muff and A. Caflisch, The Journal of Physical Chemistry B **113**, 3218 (2009).

[13] M. Sarich, F. Noé, and C. Schütte, Multiscale Model. Sim. (2009).

[14] N.-V. Buchete and G. Hummer, Phys. Rev. E **77**, 4 (2008).

[15] M. R. Shirts and J. D. Chodera, J. Chem. Phys **129**, 124105 (2008).

[16] A. M. Ferrenberg and R. H. Swendsen, Phys. Rev. Lett. **63**, 1195 (1989).

[17] S. Nosé, The Journal of Chemical Physics **81**, 511 (1984).

[18] S. Kumar, J. M. Rosenberg, D. Bouzida, and R. H. Swendsen, J. Comp. Chem. **13**, 1011 (1992).

[19] E. Gallicchio, M. Andrec, A. K. Felts, and R. M. Levy, J. Phys. Chem. B **109**, 6722 (2005).

[20] A. Mitsutake, Y. Sugita, and Y. Okamoto, Biopolymers **60**, 96 (2001).

[21] J. D. Chodera, J.-H. Prinz, W. C. Swope, F. Noé, and V. S. Pande, in preparation (2009).

[22] J. D. Chodera, N. Singhal, V. S. Pande, K. A. Dill, and W. C. Swope, J. Chem. Phys **126**, 155101 (2007).

[23] F. Noé, J. Chem. Phys **128**, 244103 (2008).

[24] W. C. Swope, H. C. Andersen, P. H. Berens, and K. R. Wilson, J. Chem. Phys **76**, 637 (1982).

[25] J. D. Chodera, W. C. Swope, J. W. Pitera, C. Seok, and K. A. Dill, J. Chem. Theo. Comp. **3**, 26 (2007).

[26] N. S. Hinrichs and V. S. Pande, The Journal of Chemical Physics **126**, 244101 (2007).

[27] N. Singhal and V. S. Pande, J. Chem. Phys **123**, 204909 (2005).

[28] H. C. Andersen, J. Chem. Phys **72**, 2384 (1980).

[29] A. I. Kinchin, *Mathematical Foundations of Statistical Mechanics* (PUBLISHER, ADDRESS, 1949).

Proof that modified parallel tempering protocol generates canonical distribution

Here we prove that the modified parallel tempering protocol described in the theory section samples from the canonical stationary distribution at all temperatures.

We define stationary distributions for momenta $\boldsymbol{p}$ and coordinates $\boldsymbol{q}$ in Cartesian space $\Re^{3N}$ at inverse temperature β:

$$\begin{aligned}\pi_p(\boldsymbol{p}|\beta) &= [P(\beta)]^{-1}\, e^{-\beta T(\boldsymbol{p})} \;\; ; \;\; P(\beta) = \int d\boldsymbol{p}\, e^{-\beta T(\boldsymbol{p})} \\ \pi_q(\boldsymbol{q}|\beta) &= [Q(\beta)]^{-1}\, e^{-\beta U(\boldsymbol{q})} \;\; ; \;\; Q(\beta) = \int d\boldsymbol{q}\, e^{-\beta U(\boldsymbol{q})}\end{aligned} \tag{42}$$

where $T(\boldsymbol{p})$ denotes the kinetic energy and $U(\boldsymbol{q})$ the potential energy function. Suppose we have two replicas the current phase space points of which are denoted by $\boldsymbol{z}_1 = (\boldsymbol{q}_1, \boldsymbol{p}_1)$ and $\boldsymbol{z}_2 = (\boldsymbol{q}_2, \boldsymbol{p}_2)$, initially at equilibrium at their respective inverse temperatures β_1 and β_2, such that

$$\begin{aligned}\boldsymbol{p}_1 &\sim \pi_p(\boldsymbol{p}_1|\beta_1) \;\; ; \;\; \boldsymbol{q}_1 \sim \pi_q(\boldsymbol{q}_1|\beta_1) \\ \boldsymbol{p}_2 &\sim \pi_p(\boldsymbol{p}_2|\beta_2) \;\; ; \;\; \boldsymbol{q}_2 \sim \pi_q(\boldsymbol{q}_2|\beta_2).\end{aligned} \tag{43}$$

We now consider what happens to the distributions of $\boldsymbol{z}_1$ and $\boldsymbol{z}_2$ after an exchange attempt. Define "post-exchange attempt" coordinates and momenta for inverse tempera-

ture β_1:

$$\begin{aligned} \boldsymbol{q}_1' &\leftarrow \begin{cases} \boldsymbol{q}_1 & \text{with prob.} \quad 1-\theta(\boldsymbol{q}_1,\boldsymbol{q}_2|\beta_1,\beta_2) \quad \text{(rejected)} \\ \boldsymbol{q}_2 & \text{with prob.} \quad \theta(\boldsymbol{q}_1,\boldsymbol{q}_2|\beta_1,\beta_2) \qquad \text{(accepted)} \end{cases} \\ \boldsymbol{p}_1' &\sim \pi_p(\boldsymbol{p}_1'|\beta_1) \quad \text{(velocity randomization)} \end{aligned}$$

where the exchange acceptance probability $\theta(\boldsymbol{q}_1,\boldsymbol{q}_2|\beta_1,\beta_2)$ is given by

$$\theta(\boldsymbol{q}_1,\boldsymbol{q}_2|\beta_1,\beta_2) \;=\; \min\{1,\exp[-\beta_1 U(\boldsymbol{q}_2)-\beta_2 U(\boldsymbol{q}_1)+\beta_1 U(\boldsymbol{q}_1)+\beta_2 U(\boldsymbol{q}_2)\} \tag{44}$$

We now compute the distribution of $\boldsymbol{q}_1'$, the configuration supposedly at temperature β_1 after the exchange attempt:

$$\begin{aligned} \rho_1(\boldsymbol{q}_1') &= \int d\boldsymbol{q}_2\,[1-\theta(\boldsymbol{q}_1',\boldsymbol{q}_2|\beta_1,\beta_2)]\,\pi_q(\boldsymbol{q}_1'|\beta_1)\,\pi_q(\boldsymbol{q}_2|\beta_2) + \int d\boldsymbol{q}_2\,\theta(\boldsymbol{q}_2,\boldsymbol{q}_1'|\beta_1,\beta_2)\,\pi_q(\boldsymbol{q}_2|\beta_1)\,\pi_q(\boldsymbol{q}_1'|\beta_2) \\ &= \int d\boldsymbol{q}_2\,[1-\min\{1,e^{-\beta_1 U(\boldsymbol{q}_2)}\,e^{-\beta_2 U(\boldsymbol{q}_1')}\,e^{+\beta_1 U(\boldsymbol{q}_1')}\,e^{+\beta_2 U(\boldsymbol{q}_2)}\}]\,\frac{e^{-\beta_1 U(\boldsymbol{q}_1')}}{Q(\beta_1)}\,\frac{e^{-\beta_2 U(\boldsymbol{q}_2)}}{Q(\beta_2)} \\ &+ \int d\boldsymbol{q}_2\,\min\{1,e^{-\beta_1 U(\boldsymbol{q}_1')}\,e^{-\beta_2 U(\boldsymbol{q}_2)}\,e^{+\beta_1 U(\boldsymbol{q}_2)}\,e^{+\beta_2 U(\boldsymbol{q}_1')}\}\,\frac{e^{-\beta_1 U(\boldsymbol{q}_2)}}{Q(\beta_1)}\,\frac{e^{-\beta_2 U(\boldsymbol{q}_1')}}{Q(\beta_2)} \\ &= \frac{e^{-\beta_1 U(\boldsymbol{q}_1')}}{Q(\beta_1)} - \min\left\{\frac{e^{-\beta_1 U(\boldsymbol{q}_1')}}{Q(\beta_1)},\frac{e^{-\beta_2 U(\boldsymbol{q}_1')}}{Q(\beta_1)}\frac{Q(\beta_1)}{Q(\beta_2)}\right\} + \min\left\{\frac{e^{-\beta_2 U(\boldsymbol{q}_1')}}{Q(\beta_2)},\frac{e^{-\beta_1 U(\boldsymbol{q}_1')}}{Q(\beta_2)}\frac{Q(\beta_2)}{Q(\beta_1)}\right\} \\ &= \pi_q(\boldsymbol{q}_1'|\beta_1) - \min\{\pi_q(\boldsymbol{q}_1'|\beta_1),\pi_q(\boldsymbol{q}_1'|\beta_2)\} + \min\{\pi_q(\boldsymbol{q}_1'|\beta_2,\pi_q(\boldsymbol{q}_1'|\beta_1) \\ &= \pi_q(\boldsymbol{q}_1'|\beta_1) \end{aligned} \tag{45}$$

Therefore, after the exchange attempt, the new configuration $\boldsymbol{q}_1'$ is still at equilibrium at the inverse temperature β_1. (A similar series of steps can be applied for the temperature β_2.)

Again redrawing the momentum from a Maxwell-Boltzmann distribution at inverse temperature β_1 will, of course, not change the equilibrium distribution, and can be shown to only support the canonical distribution at inverse temperature β_1, and no other stationary distribution [28]. Evolution by Hamiltonian dynamics for any length of time does not

alter the stationary canonical distribution [29]. Therefore, the proposed protocol samples from the canonical distribution at the desired temperatures, provided sufficient time is allowed for equilibration.

Convergence of transition probabilities in Bayesian Methods

The convergence of transition probabilities from the Bayesian sampling methods is presented in figure 8 for various temperatures. Both methods converge after approximately 5000 samples.

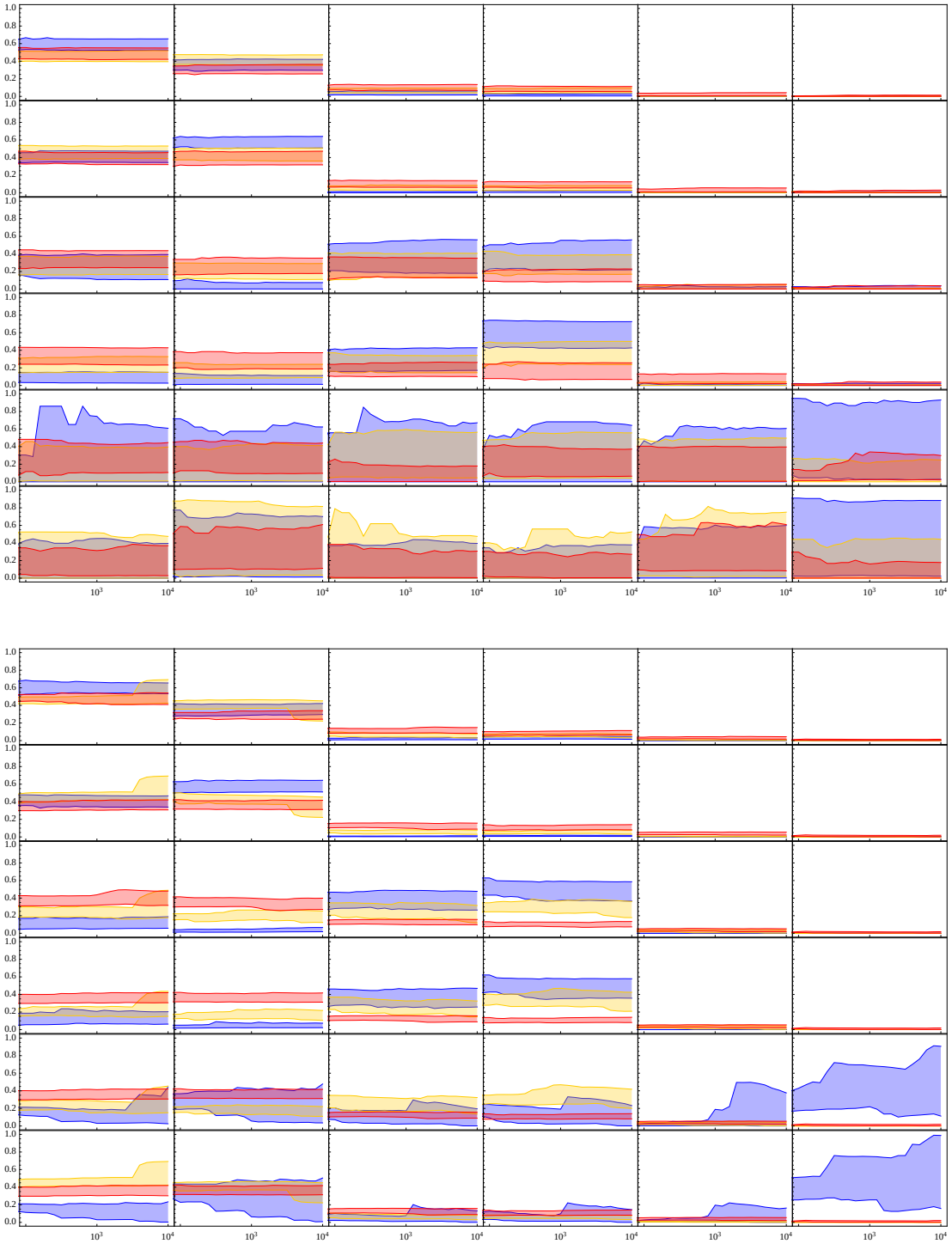

FIG. 8: 95% confidence intervals of Transition Probabilities sampled by the transition matrix estimation (upper Plot) (TE) and rate matrix estimation (lower plot) (RE) versus number of drawn samples. Color indicates performance by temperature. Blue: 273K, Yellow: 426K, Red: 600K. After about 5000 samples the confidence intervals stabilize suggesting reasonably well sampled transition probabilities.